Impaired selection of invariant natural killer T cells in diverse mouse models of glycosphingolipid lysosomal storage diseases

Stephan D. Gadola,[1] Jonathan D. Silk,[1] Aruna Jeans,[2] Petr A. Illarionov,[3] Mariolina Salio,[1] Gurdyal S. Besra,[3] Raymond Dwek,[2] Terry D. Butters,[2] Frances M. Platt,[2] and Vincenzo Cerundolo[1]

[1]Weatherall Institute of Molecular Medicine, Tumour Immunology Group, John Radcliffe Hospital, Oxford OX3 9DS, England, UK
[2]Glycobiology Institute, Department of Biochemistry, University of Oxford, Oxford OX1 3QU, England, UK
[3]School of Biosciences, University of Birmingham, Birmingham B15 2TT, England, UK

Glycolipid ligands for invariant natural killer T cells (*i*NKT cells) are loaded onto CD1d molecules in the late endosome/lysosome. Accumulation of glycosphingolipids (GSLs) in lysosomal storage diseases could potentially influence endogenous and exogenous lipid loading and/or presentation and, thus, affect *i*NKT cell selection or function. The percentages and frequency of *i*NKT cells were reduced in multiple mouse models of lysosomal GSL storage disease, irrespective of the specific genetic defect or lipid species stored. Reduced numbers of *i*NKT cells resulted in the absence of cytokine production in response to α-galactosylceramide (α-GalCer) and reduced *i*NKT cell–mediated lysis of wild-type targets loaded with α-GalCer. The reduction in *i*NKT cells did not result from defective expression of CD1d or a lack of antigen-presenting cells. Although H-2 restricted $CD4^+$ T cell responses were generally unaffected, processing of a lysosome-dependent analogue of α-GalCer was impaired in all the strains of mice tested. These data suggest that GSL storage may result in alterations in thymic selection of *i*NKT cells caused by impaired presentation of selecting ligands.

CORRESPONDENCE
Vincenzo Cerundolo:
vincenzo.cerundolo@imm.ox.ac.uk

Abbreviations used: α-GalCer, α-galactosylceramide; BMDC, bone marrow–derived DC; Gal(1→2)GalCer, galactosyl(α1→2) galactosylceramide; GSL, glycosphingolipid; iGb3, isoglobotrihexosylceramide; *i*NKT cells, invariant natural killer T cells; LOTS, late-onset Tay-Sachs disease; NPC1, Niemann-Pick disease type C1.

Presentation of glycosphingolipid (GSL) antigens via highly conserved, β2-microglobulin–associated CD1d molecules has recently been shown to exert important regulatory immune functions in mouse and man (1, 2). These effects are mediated by invariant natural killer T cells (*i*NKT cells), a highly specialized subset of CD1d-restricted T lymphocytes that are characterized by their use of an invariant TCR α chain and expression of markers specific for NK cells (3).

Human and mouse CD1d molecules can bind a diverse range of endogenous lipid ligands, including GSLs (4). An endogenous globoside, isoglobotrihexosylceramide (iGb3), has recently been shown to activate both human and mouse *i*NKT cells (5, 6). Synthetic α-galactosylceramide (α-GalCer), originally isolated from a marine sponge, is widely used for in vitro and in vivo experiments of *i*NKT cell function for its ability to stimulate *i*NKT cells in a CD1d- and TCR-dependent manner. Studies in germ-free mice, CD1d-deficient mice ($CD1d^{-/-}$), and with human cord blood indicate that *i*NKT cells are positively selected via endogenous antigens (7, 8). For presentation to *i*NKT cells, these antigens are loaded in an apparently saposin-dependent process onto CD1d molecules within the late endosome/lysosome (9, 10).

Late endocytic and lysosomal compartments are the major intracellular sites of enzymatic GSL degradation. Inherited deficiencies of lysosomal hydrolases or one of their cofactors give rise to human sphingolipid storage diseases, which are characterized by the intracellular

S.D. Gadola, J.D. Silk, and A. Jeans contributed equally to this work.
S.D. Gadola's current address is Clinic for Rheumatology and Clinical Immunology/Allergology, University Hospital of Bern, CH-3010 Bern, Switzerland.
F.M. Platt and A. Jeans's current address is Dept. of Pharmacology, University of Oxford, Oxford OX1 3QT, England, UK.
The online version of this article contains supplemental material.

Table I. Mouse models of human GSL storage disease

Disease	Lifespan	Defect	Major storage GSLs
Tay-Sachs	2 yr	β-hexosaminidase A	Minor storage of GM2 and GA2
[a]LOTS	2 yr	β-hexosaminidase A	GM2 and GA2
Sandhoff	4–5 mo	β-hexosaminidase A/B	GM2, GA2, and globoside
Fabry	2 yr	α-galactosidase A	Gb3
GM1 gangliosidosis	7–9 mo	β-galactosidase	GM1 and GA1
[b]NPC1	2.5 mo	NPC1 protein	GM2, GM3, GlcCer, and LacCer

[a]LOTS mice become symptomatic at 6–12 mo but live to 2 yr (reference 32). The Tay-Sachs mice typically remain healthy until 2 yr.
[b]NPC1 is a transmembrane protein of the late endosome/lysosome, not a catabolic enzyme, in contrast with the enzyme deficiencies that characterize the other diseases.

accumulation of storage lipids within lysosomes (11, 12). We reasoned that loading of endogenous *i*NKT cell ligands onto CD1d within late endocytic compartments could be defective in lysosomal GSL storage disease. This could arise as a result of the entrapment of endogenous ligands within membranous cytoplasmic storage bodies or as a result of these ligands being out-competed by storage lipids for binding to CD1d. To test this hypothesis, we have studied the frequency, function, and selection of *i*NKT cells in multiple independent mouse models of GSL storage. These include the GM1 gangliosidosis model (deficient in β-galactosidase) and a Niemann-Pick disease type C1 (NPC1) model. NPC1 does not result from mutations in a lysosomal enzyme or cofactor but from defects in the NPC1 transmembrane protein of the late endosome/lysosome, which is currently of unknown function. In NPC1, there is a block in the egress of cholesterol and some sphingolipids from the late endosome (13). These diseases, therefore, have radically different etiologies and display disease-specific patterns of GSL storage (14). In this paper we show that *i*NKT cells are deficient in GSL storage models irrespective of the disease-specific defect, and we discuss potential mechanisms.

RESULTS

Deficiency of *i*NKT cells in diverse mouse models of GSL storage disease

Selection of *i*NKT cells occurs through interaction with CD1d molecules presenting endogenous GSLs (15). The aberrant accumulation of GSLs in the lysosome in storage diseases therefore has the potential to negatively affect this process. We have investigated several GSL storage disease models that differ in terms of their primary etiology and store GSLs from different branches of the GSL catabolic pathway (Table I) (14).

We determined the percentage of *i*NKT cells in the thymus, spleen, and liver of different GSL storage mice and controls using CD1d tetramers loaded with the synthetic *i*NKT cell ligand α-GalCer. The organ-specific flow cytometry data are summarized for all models tested in Fig. 1 and Fig. S1 (available at http://jem.org/cgi/content/full/jem.20060921/DC1). In the mouse models of Sandhoff, GM1 gangliosidosis, Fabry, late-onset Tay-Sachs disease (LOTS), and NPC1, there was a significant reduction in the percentage of *i*NKT cells across all organs tested (ranging from a 50 to 90% reduction, depending on the model and organ; Fig. 1). Tay-Sachs mice showed a reduction in liver but not in the spleen or thymus. This mouse model has low levels of GM2 and GA2 storage relative to the other models and a normal life expectancy (Table I). We confirmed these results by examining *i*NKT cells as a percentage of total lymphocytes and the total cell number from the spleen and thymus from Sandhoff, GM1 gangliosidosis, NPC1, and Fabry mice. These data show a reduction in the *i*NKT cells as both a percentage of total lymphocytes and as absolute numbers in each model tested (Fig. S1). In contrast, the NPC1$^{+/+}$ thymic *i*NKT cell population was larger than that of other control animals. The percentage of *i*NKT cells detected in the liver of NPC1 control mice (NPC1$^{+/+}$), which are on a BALB/c background, was reduced relative to the controls of the other models that are on a C57BL/6 background. However, there

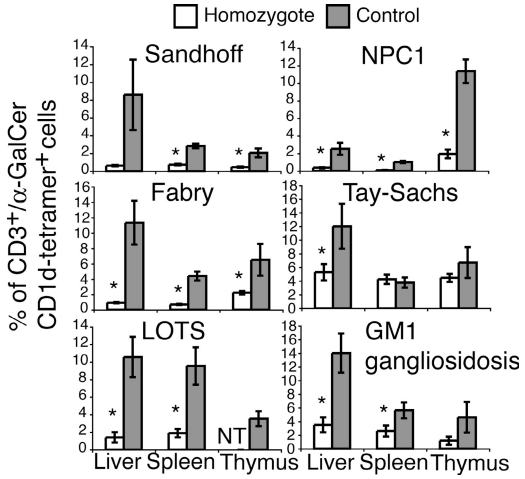

Figure 1. The percentage of *i*NKT cells is reduced in the majority of mouse models of GSL storage disease tested. Splenocytes, thymocytes, and purified liver lymphocytes from homozygous Sandhoff, NPC1, Fabry, Tay-Sachs, LOTS, and GM1 gangliosidosis mice were analyzed by flow cytometry for the presence of *i*NKT cells. Cells were stained with CD3 and α-GalCer/CD1d tetramer. The percentage of CD3$^+$/tetramer$^+$ cells (mean ± SE; n = 4–8 animals/group) from homozygous GSL storage disease animals were compared with those from control animals. Statistical significance between GSL storage disease and controls (using the t test) is indicated. *, P ≤ 0.05. NT, not tested.

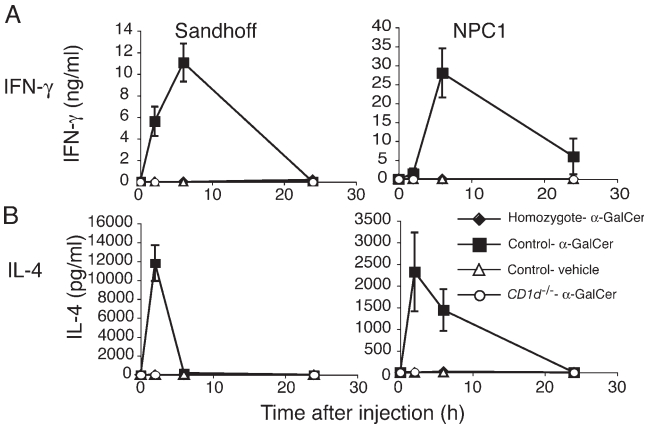

Figure 2. Cytokine release in response to injection of α-GalCer is completely abrogated in GSL storage disease mice. Homozygous Sandhoff and NPC1, wild-type, and *CD1d*$^{-/-}$ control mice were injected i.v with 1 μg α-GalCer or vehicle. Blood samples were taken at 0, 2, 6 and 24 h, and the serum was analyzed by capture ELISA for the presence of IFN-γ (A) and IL-4 (B). The data represent the mean ± SE (n = 3–4 mice/group).

was no difference in terms of absolute *i*NKT cell numbers relative to control strains (Fig. S1). Additionally, a bias toward a CD4$^+$ phenotype was observed in intrasplenic *i*NKT cells of the genetically identical Tay-Sachs and LOTS mice but not in the genetic background control mice (unpublished data).

Functional responses to α-GalCer are abrogated in GSL storage mice, whereas CD1d levels are generally unaffected

To determine whether the in vivo function of *i*NKT cells is diminished in GSL storage mice, we examined the *i*NKT-dependent response to injection of α-GalCer. Injection of α-GalCer in mice rapidly induces secretion of several different cytokines, including IL-4 and IFN-γ, into the serum (16). Although both IL-4 and IFN-γ showed normal profiles in control mice treated with α-GalCer, Sandhoff and NPC1 mice (as well as Fabry mice; unpublished data) failed to produce detectable levels of either cytokine (Fig. 2). Furthermore, in vivo cytotoxicity assays (17) demonstrated that the elimination of α-GalCer–pulsed and C20:2 analogue–pulsed wild-type targets by *i*NKT cells were severely reduced in the Sandhoff homozygote compared with control recipients (Fig. 3, B and C). These data are consistent with the low frequency of *i*NKT cells detected in these mouse models and indicate that residual *i*NKT cells are capable of antigen-specific lysis in vivo. Owing to surface loading of C20:2 onto CD1d (18), this ligand is efficiently presented by splenocytes, which results in an increase in killing efficiency observed in both wild-type and Sandhoff mice. Consistent with these observations, we demonstrated that residual *i*NKT cells from Sandhoff and GM1 gangliosidosis mice were capable of releasing IFN-γ in ELISPOT assays when stimulated by α-GalCer–pulsed bone marrow–derived DCs (BMDCs) from wild-type mice (Fig. S2, available at http://jem.org/cgi/content/full/jem.20060921/DC1). These data were confirmed by ELISA (unpublished data). Given these data, it is unlikely that the

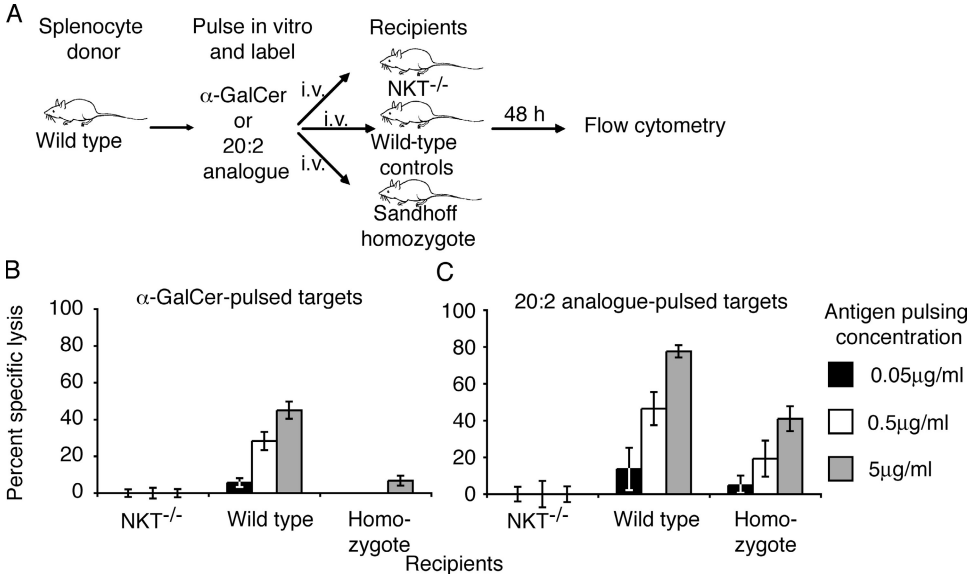

Figure 3. In vivo killing of α-GalCer–pulsed targets is reduced in GSL storage disease mice. (A) Schematic representation of the experiment. Splenocytes from wild-type donors were pulsed with α-GalCer or the C20:2 analogue and labeled with CFSE. Vehicle-pulsed targets (CMTMR labeled) were used in each case as internal controls. Target cells were injected i.v. into *i*NKT$^{-/-}$, wild-type, or Sandhoff homozygote recipients, and specific lysis was measured by flow cytometry after 48 h. Target cells were pulsed with 0.05 (black shaded), 0.5 (open), or 5 (gray shaded) μg/ml α-GalCer or C20:2 analogue. Splenocytes from wild-type donors were pulsed with α-GalCer (B) or the C20:2 analogue (C). The data represent the mean percent specific lysis (±SE; n = 3–5 mice/group) and were calculated by the formula described in Materials and methods.

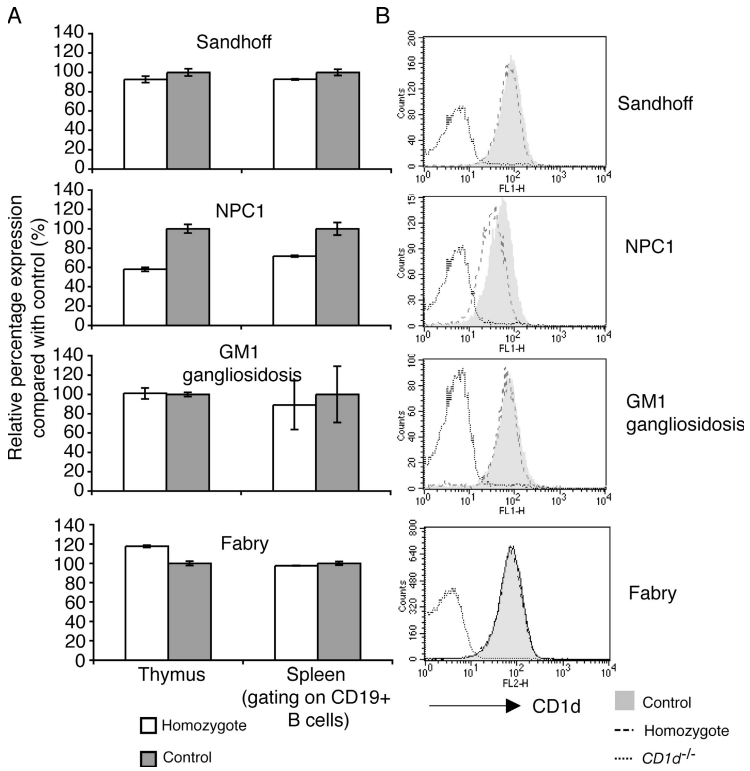

Figure 4. Cell surface expression of CD1d in GSL storage disease mice is unaffected, with the exception of NPC1 mice. Cell surface expression of CD1d on the surface of thymocytes and peripheral B cells (gating on $CD19^+$ $CD1d^{int}$ splenocytes) from Sandhoff, NPC1, GM1 gangliosidosis, Fabry, and control mice was assessed by flow cytometry. (A) Relative percentage expression (compared with controls) of CD1d cell surface level (mean ± SE; $n = 3$–5 mice/group) comparing homozygous and control mice. (B) Representative histogram overlays showing the level of CD1d expression on $CD1d^{-/-}$ (dotted line histogram), homozygote (dashed line histogram), and wild-type control (filled gray histogram) thymocytes.

residual *i*NKT cells have an inherent functional defect, but additional experiments need to be done to address this question more completely.

To further investigate the possible reasons for the reduced *i*NKT cell frequencies in GSL storage mice, we measured the cell surface CD1d expression on thymocytes and splenic B cells in GSL storage models and age-matched controls. Cell surface expression of CD1d molecules, particularly in the thymus, was not substantially altered in storage disease mice (Fig. 4, A and B; and not depicted). The only exceptions were a 40% reduction in the thymus and a 20% reduction in the spleen of NPC1 mice, and a small increase in the thymus in Fabry mice (Fig. 4, A and B).

To determine whether storage disease mice had a generalized defect in APC numbers that could contribute to the *i*NKT cell deficiency, we analyzed B cell (unpublished data), macrophage, and DC frequencies in these animals (Table II). There was a small increase in the splenic macrophage

Table II. Percentages of APCs within different disease models

	Spleen		Thymus		Liver	
	Macrophage	DC	Macrophage	DC	Macrophage	DC
C57BL/6	8.2 ± 0.5	2.5 ± 0.1	0.71 ± 0.04	0.51 ± 0.03	11.6 ± 1.9	3.1 ± 0.4
Sandhoff	[a]11.3 ± 0.8	[a]1.6 ± 0.2	0.74 ± 0.1	0.6 ± 0.02	8.7 ± 1	3.6 ± 0.5
Tay-Sachs	9.2 ± 1.2	[a]1.7 ± 0.1	0.66 ± 0.03	[a]0.64 ± 0.03	8.1 ± 0.8	[a]1.5 ± 0.4
GM1 gangliosidosis	[a]10.2 ± 0.4	[a]1.9 ± 0.1	0.95 ± 0.1	0.61 ± 0.05	9.7 ± 1	2.8 ± 0.4
Fabry	[a]10.5 ± 0.6	2.3 ± 1.1	[a]0.54 ± 0.02	0.61 ± 0.05	14 ± 2.7	3.8 ± 0.5
$NPC1^{+/+}$	4.9 ± 0.2	1.01 ± 0.02	0.44 ± 0.02	0.61 ± 0.02	12.5 ± 2.02	1.8 ± 0.2
NPC1	[a]4 ± 0.1	1.17 ± 0.07	[a]0.55 ± 0.02	[a]1.1 ± 0.13	9.22 ± 0.24	[a]3.26 ± 0.005

Cell suspensions from the various tissues were stained with antibodies against CD11c and CD68 to detect DCs and macrophages, respectively.
[a]Statistical significance between GSL storage disease and controls using the *t* test ($P \leq 0.05$).

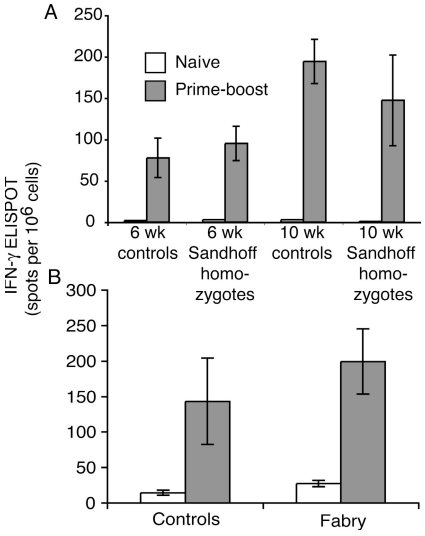

Figure 5. CD4$^+$ T cell responses are unaffected in GSL storage disease mice. (A) Sandhoff mice and controls (6 and 10 wk old) and (B) Fabry mice were primed with CFA/OVA s.c. and boosted with UV-inactivated vaccinia virus encoding full-length OVA i.v. 1 wk after boosting, splenocytes were isolated, and an overnight IFN-γ ELISPOT assay was performed using the I-A^b binding peptide $OVA_{265-280}$. Data represent the mean ± SE of the number of IFN-γ–producing spots per 10^6 cells from naive controls and prime-boosted mice (n = 3–5 mice/group).

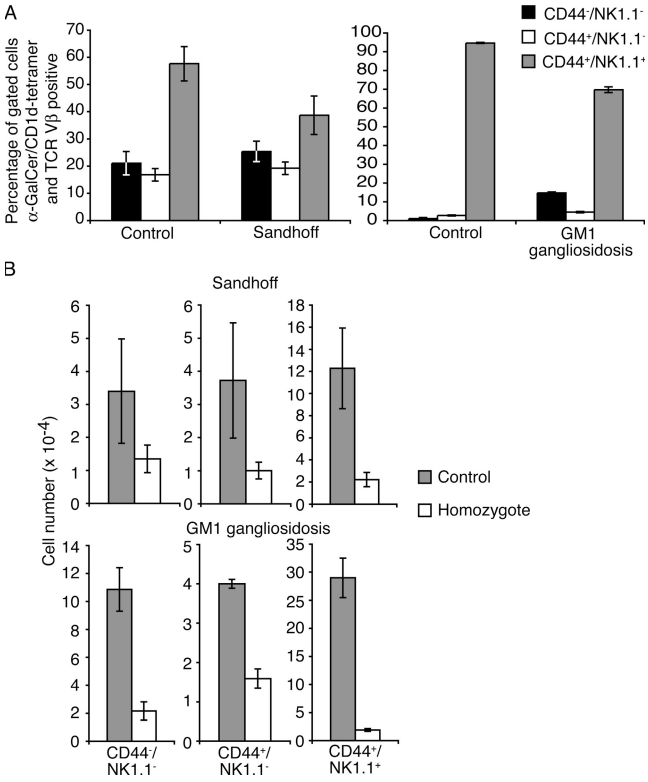

Figure 6. Selection and maturation of *i*NKT cells is compromised in the thymus of Sandhoff and GM1 gangliosidosis mice. Four-color flow cytometry was performed on thymocytes from Sandhoff, GM1 gangliosidosis, and age-matched control mice. Cells were stained with NK1.1 and CD44 antibodies, a pan–TCR Vβ antibody, and an α-GalCer/CD1d tetramer. The maturation phenotype was analyzed by gating on CD3$^+$/tetramer$^+$ cells. (A) The percentage of thymic *i*NKT cells of the immature CD44$^-$/NK1.1$^-$, semimature CD44$^+$/NK1.1$^-$, or mature CD44$^+$/NK1.1$^+$ phenotype as a percentage of α-GalCer/CD1d tetramer$^+$/Vβ$^+$ cells. (B) Total number of *i*NKT cells at three different stages of maturation (CD44$^-$/NK1.1$^-$, CD44$^+$/NK1.1$^-$, and CD44$^+$/NK1.1$^+$) from homozygous Sandhoff or GM1 gangliosidosis mice and controls are shown. Data represent one of two independent experiments (mean ± SE; n = 3–5 mice/group).

population in Sandhoff, GM1 gangliosidosis, and Fabry mice, whereas the DCs were slightly reduced in Sandhoff and GM1 gangliosidosis mice. In the thymus, there were only subtle differences in APC frequencies between GSL storage models and controls (Table II). The percentage of cortical thymocytes was generally unaffected in younger Sandhoff, GM1 gangliosidosis, and NPC1 mice, whereas a loss in *i*NKT cells in both Sandhoff and NPC1 mice was already observed at this age (unpublished data). Therefore, we conclude that the deficiency of *i*NKT cells in lysosomal GSL storage diseases is not caused by defective CD1d expression in either the thymus or periphery or a lack of CD1d$^+$ APCs.

Peptide antigen processing and presentation by MHC class II molecules are not affected by GSL storage

Processing and presentation of peptides onto MHC class II molecules is dependent on functional late endosomes/lysosomes (19). Therefore, lipid storage has the potential to disrupt these processes. We tested the capacity of Sandhoff mice to generate functional CD4$^+$ T cell responses to a model antigen, OVA. The CD4$^+$ T cell responses against two different I-A^b–binding OVA peptides, $OVA_{265-280}$ (Fig. 5 A) and $OVA_{323-339}$ (not depicted), were measured in an IFN-γ ELISPOT assay in Sandhoff and control mice. Mice were either 6 wk (before onset of neurological signs) or 10 wk of age (when the animals have a neurodegenerative phenotype). Strong OVA-specific responses of similar magnitude in Sandhoff mice (6 and 10 wk of age) and age-matched controls were detected after prime-boost immunization with OVA. These data rule out any impairment of OVA processing and presentation via MHC class II molecules. Although both Fabry (Fig. 5 B) (20) and GM1 gangliosidosis mice made class II–restricted responses, NPC1 mice had a reduced ability to generate anti-OVA responses (not depicted). Furthermore, the proportion of thymic CD4$^+$ T cells in Sandhoff and control mice were similar, which was consistent with unimpaired H-2–dependent thymic selection (unpublished data).

GSL storage affects positive selection of *i*NKT cells

Different maturation stages of *i*NKT cells have recently been defined in mice (21–23). After positive selection (24), α-GalCer/CD1d–specific thymocytes bearing the invariant TCR α chain (TCR Vα14-Jα18) sequentially express CD44 and NK1.1 molecules, respectively. To investigate whether GSL storage affects thymic development of *i*NKT cells, we analyzed the populations of *i*NKT cells at different stages of

Table III. Biochemical and cell biological consequences of GSL storage in the thymus of the Sandhoff disease mouse

		Control	Sandhoff	Fold elevation
HPLC analysis of GSLs	[a]GM1a	28.3 ± 2.9	24.8 ± 2.1	0.89
	[a]GM1b	150.3 ± 24	133.7 ± 15.8	0.89
	[a]GA1	121.7 ± 12.6	118.6 ± 12.8	0.97
	[a]GM2	8.3 ± 1.5	[b]17.9 ± 3.8	2.15
	[a]GA2	34 ± 4.89	[b]166.9 ± 24.8	4.91
	[a]GM3	5.8 ± 1.05	[b]2.14 ± 0.75	0.36
Flow cytometry	[c]LysoTracker	100 ± 5.3	[b]211.3 ± 21.3	2.11

[a]Levels of GSL species in total thymic extract from 10–12-day-old Sandhoff and control mice (pg/mg protein), as determined by HPLC (reference 41).
[b]Statistical significance using the *t* test ($P \leq 0.05$).
[c]A relative measure of the total acidic late endosomal/lysosomal compartment was made using LysoTracker staining. Flow cytometry was used to analyze LysoTracker-stained thymocytes (relative fluorescence intensity), gating on the lymphoid population using forward and side scatter parameters.

thymic maturation in Sandhoff and GM1 gangliosidosis mice and controls (Fig. 6 A). The different *i*NKT cell populations observed in age-matched control mice were similar to previous reported data (25). The majority of thymic *i*NKT cells were of the "mature" $CD44^+/NK1.1^+$ phenotype, with subpopulations of the "semimature" $CD44^+/NK1.1^-$ and "immature" $CD44^-/NK1.1^-$ cells. All three maturation stages could be clearly identified in both strains of mice (percent of gated $tetramer^+/TCR^+$ cells; Fig. 6 A). However, both Sandhoff and GM1 gangliosidosis mice exhibited a striking reduction in absolute numbers of α-GalCer/CD1d–specific thymocytes at all three stages of development studied (Fig. 6 B), culminating in the most significant reduction at the mature $CD44^+/NK1.1^+$ stage. These results are consistent with impaired thymic-positive selection of *i*NKT cells caused by GSL storage.

To further analyze whether thymocytes, necessary for the positive selection of *i*NKT cells (15), display inappropriate GSL accumulation in Sandhoff mice, we performed quantitative analysis of the levels of GSL storage in total thymus. As shown in Table III, the levels of GM2 and GA2 were significantly elevated in 10–12-d-old Sandhoff thymus compared with age-matched controls, whereas the level of GM3 was reduced. As expected, the levels of GM1a, GM1b, and GA1, not substrates for β-hexosaminidase A/B, were unchanged.

It is known that macrophages accumulate considerable levels of GSLs within late endosomes/lysosomes in Sandhoff disease (unpublished data). Therefore, it was possible that the storage of GSLs observed in the thymus (Table III) was caused by resident macrophages and not thymocytes. To determine whether GSLs are also stored in thymocytes, we examined the size/number of lysosomes in thymocytes using LysoTracker staining. (Table III). We found that the relative fluorescence intensity of staining was significantly elevated in Sandhoff thymocytes compared with wild-type controls. An increase in the number and/or size of lysosomes within these cells suggests that thymocytes are storing GSLs. Collectively, these data suggest that accumulation of GSLs within late endosomes/lysosomes in thymocytes may impair selection of *i*NKT cells in Sandhoff mice.

Impaired presentation of exogenous ligands by GSL storage APCs

To further examine the mechanism for the loss of *i*NKT cells in the different GSL storage disease mice, we performed experiments using α-GalCer and an analogue that requires endosomal processing to stimulate *i*NKT cells (5, 20). This was done to determine whether APCs from GSL storage disease mice had a defect in the capacity to load CD1d with ligands in the lysosome.

Sandhoff, GM1 gangliosidosis, Fabry, or NPC1 splenocytes or BMDCs were pulsed with α-GalCer (Fig. 7, A and C; and not depicted) and used to stimulate an *i*NKT cell hybridoma (DN32-D3), or left unpulsed and used to stimulate a control, CD1d-restricted, noninvariant NKT cell hybridoma (TCB11; Fig. 7, E and F). Splenocytes from both Sandhoff and GM1 gangliosidosis mice appeared to be defective in presenting α-GalCer to the DN32 hybridoma compared with wild-type controls (Fig. 7 A). Interestingly, the defect in ability to present α-GalCer observed with Sandhoff and GM1 gangliosidosis splenocytes is not apparent when the APCs used were cultured BMDCs (Fig. 7 C).

We also examined the capacity of APCs from GSL storage disease mice to process and present an analogue of α-GalCer that is strictly dependent on lysosomal processing, galactosyl(α1→2) galactosylceramide (Gal(1→2)GalCer) (5, 20). This analogue has a second galactose group linked to the primary galactose of α-GalCer and requires processing by α-galactosidase (deficient in Fabry disease) within the lysosome, before recognition in the context of CD1d can occur. It has previously been shown that Fabry mice are unable to process and present Gal(1→2)GalCer (20).

These experiments were performed using splenocytes (Fig. 7 B) or BMDCs (Fig. 7 D) from Sandhoff and GM1 gangliosidosis mice, as well as NPC1 mice (unpublished data). The response of the DN32 hybridoma to splenocytes or BMDCs from Sandhoff and GM1 gangliosidosis mice pulsed with Gal(1→2)GalCer was reduced compared with wild-type controls but was greater than that seen with $CD1d^{-/-}$ APCs. Similarly, NPC1 mice had a dramatically reduced capacity to present Gal(1→2)GalCer (unpublished data).

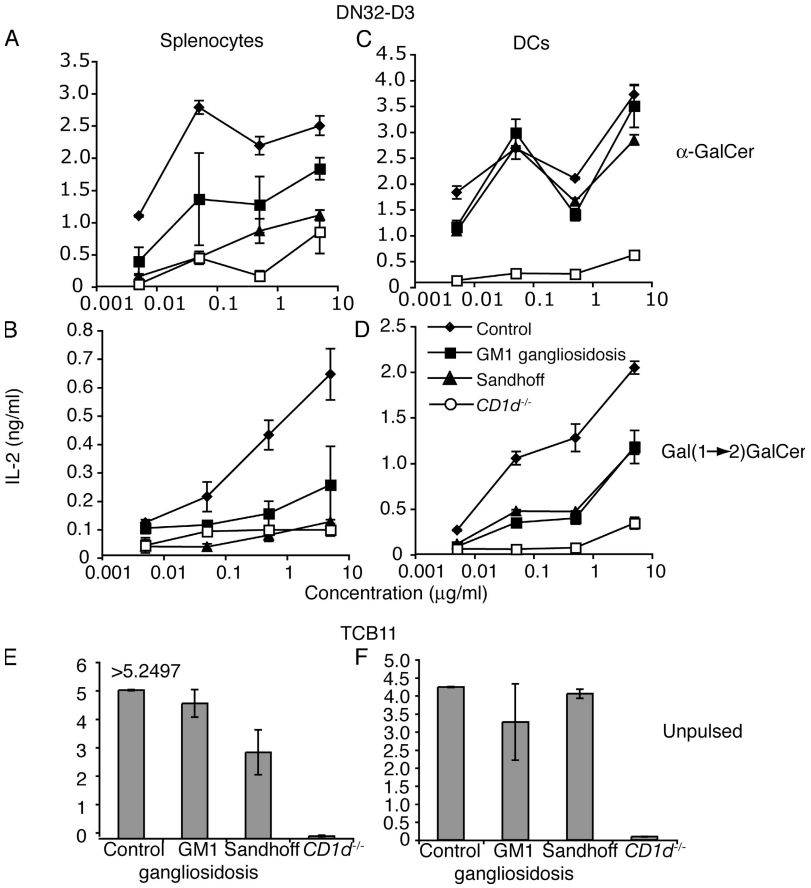

Figure 7. Reduced capacity to process and present a lysosome-dependent analogue of α-GalCer by GSL storage APCs. Splenocytes (A, B, and E) and TNF-α–matured BMDCs (C, D, and F) from control, GM1 gangliosidosis, Sandhoff, or CD1dKO mice were pulsed for 6 h with either α-GalCer (A and C) or Gal(1→2)GalCer (B and D) and used to stimulate the DN32-D3 invariant NKT cell hybridoma (A, B, C, and D). Unpulsed splenocytes (E) and BMDCs (F) were used to stimulate the CD1d-restricted, noninvariant hybridoma TCB11 for 24 h in vitro. Supernatants were analyzed using an IL-2 ELISA. Data represent one of two independent experiments (mean ± SE; $n = 2$–3 mice/group).

DISCUSSION

In this study, we investigated a broad range of GSL storage disease models, including the NPC1 mouse, which, in contrast to the other diseases, has no defect in the catabolic enzymes of the lysosome. Specifically, we have studied mouse models of GM2 gangliosidosis (Tay-Sachs, LOTS, and Sandhoff), GM1 gangliosidosis, Fabry, and NPC1. The major storage lipids for each of these models are listed in Table I. The only common feature shared by these diseases is the accumulation of GSLs in the late endosome/lysosome.

Characterization of *i*NKT cell frequencies in GSL storage disease mice

We have found that *i*NKT cells are present at reduced percentages and frequencies in all mouse models tested, irrespective of the specific GSLs stored, and in all organs studied (Fig. 1 and Fig. S1). The only exception was the Tay-Sachs mouse, in which *i*NKT cells were reduced in the liver but normal in the thymus and spleen. This mouse stores only modest levels of GM2/GA2 (in contrast with the LOTS and Sandhoff mice) because of a compensatory pathway and does not typically develop clinical neurological signs within its normal life span (14). It is interesting to note that GSL storage is not detectable in thymus or spleen of Tay-Sachs mice, whereas there is a fivefold elevation of GA2 in the liver (Priestman, D., personal communication), implying that GA2 storage alters the liver microenvironment, affecting *i*NKT cell homeostasis. Disease-dependent variations in organ-specific GSL profiles may explain subtle differences in *i*NKT cell frequencies in the different models. Furthermore, the lack of GSL storage and normal *i*NKT cell frequency observed in the Tay-Sachs mouse indicates that a threshold level of thymic storage may be required to impair *i*NKT cell development.

Functional characterization of residual *i*NKT cells

In view of the fact that *i*NKT cells were not completely absent, it raised the issue as to whether the residual cells were functional. In Sandhoff and NPC1 mice there was undetectable cytokine release in response to α-GalCer injection, relative to controls (Fig. 2). These results are consistent with

previously published papers (5, 26) demonstrating a reduction in *i*NKT cell frequencies in Sandhoff and NPC1 mice. The complete absence of a cytokine response in the storage disease mice suggests that if the residual *i*NKT cells are functional, the levels of cytokines released are below the detection limit of the assays. Alternatively, they may be defective and incapable of responding. In addition, GSL storage disease APCs may inefficiently present α-GalCer. To investigate the functional capacity of the residual *i*NKT cells, in vivo killing of wild-type α-GalCer–pulsed and C20:2 analogue–pulsed (18) targets was assessed in Sandhoff mice (Fig. 3, B and C). As predicted, the specific lysis was reduced (as a result of the reduction in *i*NKT cells). However, there was detectable killing (Fig. 3 C) and IFN-γ production (Fig. S2), suggesting that the residual *i*NKT cells are capable of responding to antigen-pulsed wild-type targets. To address the function of residual *i*NKT cells, it would be useful to use intracellular cytokine staining on individual cells. However, in our hands this technique was insufficiently sensitive for this purpose (unpublished data). Whether residual *i*NKT cells in Sandhoff or GM1 gangliosidosis mice are defective—compared with controls—on a per cell basis remains thus unclear.

The role of CD1d expression

In agreement with published studies of the Sandhoff and prosaposin knockout mouse models (5, 27), levels of cell surface CD1d were generally unchanged in GSL storage disease mice (Fig. 4). Of note, the level of CD1d was reduced on thymocytes and B cells in the NPC1 mouse (Fig. 4). These data suggest that the complex pattern of storage lipids in NPC1 and/or the block in trafficking from the late endosome that occurs in this disease partially suppresses cell surface CD1d expression. However, as all other mouse models tested did not exhibit reduced CD1d expression, it is unlikely that the decreased CD1d levels in NPC1 mice are entirely responsible for the reduction in *i*NKT cells.

Processing and presentation within the lysosome

Although presentation of peptides by MHC class II molecules is unaffected in the different disease mouse models (with the exception of NPC1 ; Fig. 5), processing and presentation of endogenous or exogenous GSL antigens may be affected by GSL storage. To test whether presentation of exogenous GSLs was compromised, we used APCs from Sandhoff, GM1 gangliosidosis, NPC1, and control mice—loaded with either α-GalCer or an analogue, Gal(1→2)GalCer (20)—to stimulate a $V\alpha14^+$ *i*NKT cell hybridoma (27). In these experiments, CD1d presentation of both α-GalCer (partially dependent on lysosomal loading) and Gal(1→2)GalCer (strictly dependent on lysosomal processing and loading) (20) was impaired in splenocytes from Sandhoff, GM1 gangliosidosis (Fig. 7, A and B), and NPC1 mice (not depicted). The response of the TCB11 control hybridoma was similar between mouse strains (Fig. 7, E and F).

Experiments performed using Sandhoff- and GM1 gangliosidosis–cultured BMDCs confirmed reduced presentation of Gal(1→2)GalCer, as compared with presentation by control BMDCs (Fig. 7 D). In contrast with splenocytes, BMDCs from Sandhoff and GM1 gangliosidosis mice were capable of efficiently presenting α-GalCer (Fig. 7, A and C). Collectively, these data suggest that the accumulation of GSL in the lysosome can impair lysosomal processing and/or loading of CD1d ligands for presentation to *i*NKT cells. In addition, the defect in sphingolipid trafficking observed in all models (28) may contribute to the reduction in exogenous ligand presentation. GSL storage by different GSL storage disease model BMDCs was confirmed by their elevation in LysoTracker staining (unpublished data).

The difference observed between splenocytes and BMDCs in their capacity to present exogenous α-GalCer could be explained by several factors. For example, it may reflect increased glycolipid antigen uptake/processing by an enriched population of DCs compared with splenocytes, which contains CD1d-positive macrophages and B cells as well as DCs. TNF-α–induced maturation of BMDCs could further enhance uptake and presentation of glycolipids. Alternatively, cultured BMDCs and splenocytes may differ with regard to the degree of GSL accumulation within lysosomes.

Interestingly, previously published data (5) did not find any such defect in the capacity to process and present Gal(1→2)GalCer by Sandhoff APCs. It is possible that technical differences in the experiments—such as the age of the mice and, consequently, the degree of GSL accumulation—may affect the results obtained. A more detailed analysis of the effects of age and degree of accumulation on the ability to present Gal(1→2)GalCer is currently being undertaken.

Impaired *i*NKT cell thymic selection in GSL storage mice

Processing and presentation of endogenous *i*NKT cell selecting ligands may also be affected by GSL storage. The reduction of *i*NKT cells in GSL storage mice might therefore be caused by a reduced capacity to positively select *i*NKT cells during thymic development. A reduction of *i*NKT cells at all developmental stages was observed in the thymus of young adult Sandhoff and GM1 gangliosidosis mice (Fig. 6). Interestingly, we found a significant reduction in the frequency of *i*NKT cells in Sandhoff mice at postnatal day 12 (unpublished data), when appreciable levels of GSL storage are already detected (Table III), suggesting that accumulation of GSLs in thymocytes may lead to a decreased capacity to positively select *i*NKT cells.

Loss of *i*NKT cells in mouse models characterized by lysosomal GSL accumulation has previously been described. One report (20) proposed that the loss of *i*NKT cells in Fabry mice was indicative of a requirement for α-galactosidase (the enzyme deficient in Fabry disease) for the generation of glycolipid ligands recognized by *i*NKT cells. Another group observed a reduction in *i*NKT cells in Sandhoff mice and concluded that there was an essential requirement for β-hexosaminidase A/B (the enzymes deficient in Sandhoff mice) to generate the endogenous lipid necessary for selection of *i*NKT cells (5). Of the candidate substrates tested,

iGb3 was proposed to be the selecting ligand based upon its activity in vitro. Likewise, recent studies with prosaposin-deficient mice revealed a similar reduction in *i*NKT cell frequencies, suggesting an essential role for saposins in the loading of CD1d (27). Interestingly, a paper was recently published supporting our observations of a reduction of *i*NKT cells in NPC1 mice (26).

Alternative hypothesis and potential mechanisms

Our data obtained from a range of different GSL storage models, including GM1 gangliosidosis and NPC1, support the hypothesis that lysosomal lipid storage has an independent, nonspecific negative effect on *i*NKT cell selection. In NPC1 mice, reduced *i*NKT cell frequencies may be caused by a combined effect of GSL storage, impaired GSL trafficking, and decreased CD1d expression (26). This hypothesis could also explain the finding that *i*NKT cells are reduced in Fabry mice, where the deficiency in α-galactosidase A should lead to lysosomal accumulation of iGb3, the recently identified candidate endogenous ligand for *i*NKT cells.

We propose an alternative model to explain *i*NKT cell loss in the disparate mouse models investigated in this study and others (5, 20, 26, 27). The storage of any GSL above a certain threshold in the late endosome/lysosome, irrespective of its structure, could impair *i*NKT cell development. It is the storage per se rather than a specific enzyme defect that results in *i*NKT cell deficiency. This model is also consistent with the *i*NKT cell reduction observed in the saposin-null mice because GSLs accumulate as a result of the saposin deficiency. In addition, lack of lipid solubilization (29) mediated by saposins may further impair the loading of CD1d with endogenous *i*NKT cell selecting ligands. Therefore, saposin-deficient mice suffer from the combined effects of GSL storage and reduced GSL loading. This may also explain why residual *i*NKT cells are detectable in the Fabry, Sandhoff, GM1 gangliosidosis, and NPC1 mice (GSL storage), whereas they are undetectable in the saposin-deficient animals (GSL storage and loading defect).

There are several potential mechanisms to envision for how GSL storage affects CD1d loading. The first would be that endogenous GSLs normally presented by CD1d become trapped within the storage bodies in the diseased cells and consequently are not loaded onto CD1d. A second hypothesis would be that the high levels of storage GSLs outnumber natural ligands within the late endosome/lysosome and, therefore, out-compete the endogenous lipids for binding to CD1d. Both of these models are consistent with a threshold level of storage being required to disrupt *i*NKT cell development. This is supported by the intermediate *i*NKT cell loss exhibited by the Tay-Sachs mouse (Fig. 1) that has subpathological levels of GSL storage (Table I). Alternatively, GSL storage may indirectly influence *i*NKT cell selection. The defect in sphingolipid trafficking (27) observed in all GSL storage disease models may disrupt the cellular distribution of the selecting ligands, reducing their presentation by CD1d and *i*NKT cell selection. The proposed mechanisms by which GSL storage disrupts *i*NKT cell selection are not mutually exclusive and, therefore, we cannot rule out that this also plays a role.

It will be interesting to determine whether comparable *i*NKT cell deficiencies occur in patients with glycosphingolipidoses. Although these studies are currently in progress, a recent report has described that Gaucher patients (who possess a defect in the lysosomal enzyme glucocerebrosidase) treated with enzyme replacement therapy showed a modest increase in the proportion of $V\alpha24^+$ cells in the peripheral $CD4^+$ and $CD8^+$ T cell pool (30). Should the findings of our study translate to the human disorders, *i*NKT cell deficiency may be a contributing factor to the clinical heterogeneity characteristic of these diseases. It is possible that this may have consequences for host immune responses by reducing the efficacy of presentation of bacterial or endogenous GSLs.

In summary, storage of multiple GSLs with disparate structures, resulting from unique etiologies, causes defective *i*NKT cell selection. Our data suggest general mechanisms by which lysosomal storage of GSLs, irrespective of the underlying gene defect, can disrupt the presentation of endogenous ligands by CD1d.

MATERIALS AND METHODS

Animals. The following mouse models of GSL storage (C57BL/6 background) were maintained and genotyped according to published methods: Tay-Sachs $hexa^{-/-}$ (31); LOTS $hexa^{-/-}$ (32); Sandhoff $hexb^{-/-}$ (33); Fabry $\alpha\text{-}galA^{-/-}$ (34); and GM1 gangliosidosis $bgal^{-/-}$ (35). Each mouse strain had been backcrossed at least eight times before use. LOTS mice are female Tay-Sachs mice that have been repeatedly bred before 6 mo of age (32). Tay-Sachs (nonbred) mice are asymptomatic because of the presence of a bypass pathway (the combined effects of sialidase and hexosaminidase B). Pregnancy induces down-regulation of components of the bypass pathway, causing higher levels of storage relative to the Tay-Sachs mouse and clinical presentation in 100% of LOTS mice. NPC1 mice (13) are on a BALB/c background. Also used were mice lacking the Jα18 TCR gene segment (36), which were devoid of Vα14 *i*NKT cells while having other lymphoid cell lineages intact ($i\text{NKT}^{-/-}$ mice), and CD1d knockout mice ($CD1d^{-/-}$) (37), which were also devoid of Vα14 *i*NKT cells. Heterozygote littermates and age-matched C57BL/6 or $NPC1^{+/+}$ mice, as appropriate, were used as controls. All mice were maintained in the Biological Services Unit, Department of Biochemistry, University of Oxford and used according to established University of Oxford institutional guidelines under the authority of a UK Home Office project license.

Cell preparations. Intrahepatic mononuclear cells were separated from mouse livers according to the following protocol: livers were cut into small pieces using a scalpel, passed through a 100-mm metal mesh filter, washed twice with PBS, layered over Ficoll-Hypaque gradients, and centrifuged at 2,000 rpm at room temperature for 20 min. An analogous procedure was used to separate splenic and thymic mononuclear cells. Before staining for FACS, both intrahepatic and splenic mononuclear cells were incubated for 10 min at room temperature with 20 μg of unconjugated anti-FcR antibody (BD Biosciences). For all FACS staining experiments, three to five animals per group were used.

Flow cytometry. Cell suspensions were stained according to published methods (38). In brief, 10^6 cells in 50 μl FACS buffer (PBS containing 1% bovine serum albumin and 0.02 M sodium azide) were incubated on ice for 30 min with monoclonal antibodies (all from BD Biosciences) or α-GalCer/CD1d tetramer (39), followed by two washes in FACS buffer. The antibodies used were R-phycoerythrin (RPE)–conjugated rat anti–mouse CD1d

(CD1.1, Ly-38), FITC-conjugated rat anti–mouse CD19 (1D3), hamster anti–mouse CD11c (HL3), and CD68. Allophycocyanin-conjugated streptavidin (Phykolink) and RPE-conjugated Extraavidin (Sigma-Aldrich) were used for the generation of CD1d tetramers. CD1d tetramers were generated as previously described (39). Propidium iodide was used to gate out dead cells. Quantitation of binding sites was performed using fluorescent microbead standards according to published methods (38). To analyze the maturation phenotype of *i*NKT thymocytes, cells were stained with CD1d/α-GalCer tetramer–PE, NK1.1-PerCP, pan Vβ–FITC, and CD44-allophycocyanin (BD Biosciences). To analyze lysosomes, 10^6 cells from 10–12-d-old Sandhoff and control thymi were stained in 200 μl 200 nM LysoTracker-Green (Invitrogen) for 10 min at room temperature. After washing, the cells were analyzed by flow cytometry gating on thymocytes by forward and side scatter. Percentages of APCs were analyzed by staining cells from different tissues with CD11c and CD68 antibodies.

Cytokine assays. Animals were injected i.v. with 1 μg α-GalCer (dissolved in a vehicle solution of 0.5% Tween 20/PBS) or vehicle diluted in PBS. Blood samples were collected at the time points indicated in the figures, and serum levels of IL-4 and IFN-γ were determined using cytokine-specific capture ELISAs. Antibodies used for ELISAs were obtained from eBioscience and Pierce Chemical Co.

In vivo cytotoxicity assay. Target splenocytes were pulsed with 5, 0.5, and 0.05 μg/ml α-GalCer or C20:2 analogue for 2 h at 37°C and labeled with different concentrations (1.65, 0.3, and 0.07 nM) of CFSE (Invitrogen), as previously described (17). A control vehicle-pulsed population was labeled with 10 μM chloromethyl-benzoyl-aminotetramethyl-rhodamine (CMTMR; Invitrogen). An equal mixture of the four populations of splenocytes was injected i.v. at 10^7 cells/mouse into Sandhoff homozygote mice, age-matched littermate controls, and *i*NKT$^{-/-}$ mice ($n = 3$–5 mice/group). 48 h after injection, blood samples were examined for the presence of fluorescent cells by flow cytometry (FACSCalibur; BD Biosciences). Data are expressed as percent survival of α-GalCer– or analogue-pulsed splenocytes compared with unpulsed controls. Mean percent specific lysis (±SEM) of α-GalCer–pulsed splenocytes compared with unpulsed controls was calculated by the following formula: $100 - ([\text{pulsed/unpulsed}] \times 100)$.

Monitoring MHC class II–restricted T cell responses. Sandhoff homozygotes (6 and 10 wk of age) or other GSL storage mice and age-matched controls were immunized s.c. with 100 μg chicken OVA protein (Sigma-Aldrich) in CFA (Sigma-Aldrich). 11 d later, the mice were injected i.v. with 2×10^6 PFU/mouse UV-inactivated recombinant vaccinia virus encoding full-length chicken OVA. After 7 d, immune responses were assessed by performing ELISPOT using a mouse IFN-γ ELISPOT kit (Mabtech) and 10 μM of two different I-A^b–restricted OVA peptides (synthesized in house), $OVA_{265\text{-}280}$ (TEWTSSNVMEERKIKV) and $OVA_{323\text{-}339}$ (ISQAVHAAHAEINEAGR), according to the manufacturer's protocol.

Analysis of GSL storage. Thymi from 10–12-d-old Sandhoff mice and controls were homogenized in 0.5 ml distilled water, and GSLs were extracted using the Svernnerholm method (40). The equivalent of 200 μg protein was treated with ceramide glycanase (Calbiochem-Novabiochem). Released glycans were labeled with anthranillic acid (Sigma-Aldrich) and analyzed by HPLC as described previously (41).

Processing and presentation of α-GalCer and analogues by GSL storage disease APCs. APCs used were either BMDCs, cultured for 7 d in the presence of 20 ng/ml GM-CSF/IL-4 (PeproTech) and matured from day 6 of culture with 10 ng/ml TNF-α (PeproTech) or splenocytes. APCs were pulsed with α-GalCer, Gal(1→2)GalCer, or vehicle for 6 h, washed, and 5×10^5 splenocytes or 5×10^4 BMDCs were added to 96-well flatbottom plates. The DN32-D3 *i*NKT cell hybridoma or the control, CD1d-restricted, non–*i*NKT cell hybridoma (TCB11) from A. Bendelac (University of Chicago, Chicago, IL) and S. Porcelli (Albert Einstein School of Medicine, New York, NY) were added (5×10^4) to each well. Cells were cultured for 18–24 h at 37°C, and the supernatant was analyzed for the presence of IL-2 by ELISA (antibodies used were anti–mouse IL-2 JES6-1A12 and biotinylated JES6-5H4; eBioscience).

Online supplemental material. In Fig. S1, lymphocyte preparations from the spleen and thymus were generated, and cells were counted. Lymphocytes were stained for iNKT cells as described in Flow cytometry, and samples were analyzed. The cell number and frequency of iNKT cells as a percentage of total lymphocytes were then used to calculate the number of tissue iNKT cells.

In Fig. S2, the ability of iNKT cells from storage disorder mice to mount a cytokine response was assayed by performing an overnight IFN-γ ELISPOT using T cell–enriched splenocytes incubated with BMDCs loaded with α-GalCer. Splenocyte cell preparations were enriched for T cells by incubating for 1 h at 37°C, adhering out the macrophages. BMDCs derived from wild-type mice were pulsed for 3 h with 5 μg/ml α-GalCer. Online supplemental material is available at http://www.jem.org/cgi/content/full/jem.20060921/DC1.

The authors wish to thank Dawn Shepherd, Andrea Tarlton, David Smith, and Denise Jelfs for excellent technical support; Dr. David Neville for HPLC analysis of GSL oligosaccharides; and Professor Albert Bendelac, Dr. Dapeng Zhou, and Professor Steve Porcelli for the kind gift of the hybridomas.

This work was funded by the Swiss National Science Foundation and Max Cloetta Foundation (S.D. Gadola), the Medical Research Council (grant G0400421 to V. Cerundolo and a studentship to A. Jeans), the Wellcome Trust (grant 072021/Z/03/Z), the Lister Institute for Preventive Medicine (G.S. Besra and F.M. Platt), the Glycobiology Institute, the University of Oxford (T.D. Butters and F.M. Platt) and Cancer Research UK (grant C399-A2291), and the Cancer Research Institute.

The authors have no conflicting financial interests.

Submitted: 12 May 2006
Accepted: 23 August 2006

REFERENCES

1. Taniguchi, M., M. Harada, S. Kojo, T. Nakayama, and H. Wakao. 2003. The regulatory role of Vα14 NKT cells in innate and acquired immune response. *Annu. Rev. Immunol.* 21:483–513.
2. Brigl, M., and M.B. Brenner. 2004. CD1: antigen presentation and T cell function. *Annu. Rev. Immunol.* 22:817–890.
3. Bendelac, A. 1995. CD1: presenting unusual antigens to unusual T lymphocytes. *Science.* 269:185–186.
4. Naidenko, O.V., J.K. Maher, W.A. Ernst, T. Sakai, R.L. Modlin, and M. Kronenberg. 1999. Binding and antigen presentation of ceramide-containing glycolipids by soluble mouse and human CD1d molecules. *J. Exp. Med.* 190:1069–1080.
5. Zhou, D., J. Mattner, C. Cantu III, N. Schrantz, N. Yin, Y. Gao, Y. Sagiv, K. Hudspeth, Y.P. Wu, T. Yamashita, et al. 2004. Lysosomal glycosphingolipid recognition by NKT cells. *Science.* 306:1786–1789.
6. Mattner, J., K.L. Debord, N. Ismail, R.D. Goff, C. Cantu III, D. Zhou, P. Saint-Mezard, V. Wang, Y. Gao, N. Yin, et al. 2005. Exogenous and endogenous glycolipid antigens activate NKT cells during microbial infections. *Nature.* 434:525–529.
7. Park, S.H., K. Benlagha, D. Lee, E. Balish, and A. Bendelac. 2000. Unaltered phenotype, tissue distribution and function of Vα14(+) NKT cells in germ-free mice. *Eur. J. Immunol.* 30:620–625.
8. van Der Vliet, H.J., N. Nishi, T.D. de Gruijl, B.M. von Blomberg, A.J. van den Eertwegh, H.M. Pinedo, G. Giaccone, and R.J. Scheper. 2000. Human natural killer T cells acquire a memory-activated phenotype before birth. *Blood.* 95:2440–2442.
9. Jayawardena-Wolf, J., K. Benlagha, Y.H. Chiu, R. Mehr, and A. Bendelac. 2001. CD1d endosomal trafficking is independently regulated by an intrinsic CD1d-encoded tyrosine motif and by the invariant chain. *Immunity.* 15:897–908.
10. Chiu, Y.H., S.H. Park, K. Benlagha, C. Forestier, J. Jayawardena-Wolf, P.B. Savage, L. Teyton, and A. Bendelac. 2002. Multiple defects in antigen presentation and T cell development by mice expressing cytoplasmic tail-truncated CD1d. *Nat. Immunol.* 3:55–60.

11. Schuette, C.G., T. Doering, T. Kolter, and K. Sandhoff. 1999. The glycosphingolipidoses-from disease to basic principles of metabolism. *Biol. Chem.* 380:759–766.
12. Jeyakumar, M., T.D. Butters, R.A. Dwek, and F.M. Platt. 2002. Glycosphingolipid lysosomal storage diseases: therapy and pathogenesis. *Neuropathol. Appl. Neurobiol.* 28:343–357.
13. Loftus, S.K., J.A. Morris, E.D. Carstea, J.Z. Gu, C. Cummings, A. Brown, J. Ellison, K. Ohno, M.A. Rosenfeld, D.A. Tagle, et al. 1997. Murine model of Niemann-Pick C disease: mutation in a cholesterol homeostasis gene. *Science.* 277:232–235.
14. Hopwood, J.J., A.C. Crawley, and R.M. Taylor. 2004. Spontaneous and engineered mammalian storage disease models. *In* Lysosomal Disorders of the Brain: Recent Advances in Molecular and Cellular Pathogenesis and Treatment. F. Platt and S. Walkley, editors. Oxford University Press, Oxford. 257–289.
15. Bendelac, A. 1995. Positive selection of mouse NK1$^+$ T cells by CD1-expressing cortical thymocytes. *J. Exp. Med.* 182:2091–2096.
16. Hermans, I.F., J.D. Silk, U. Gileadi, M. Salio, B. Mathew, G. Ritter, R. Schmidt, A.L. Harris, L. Old, and V. Cerundolo. 2003. NKT cells enhance CD4$^+$ and CD8$^+$ T cell responses to soluble antigen in vivo through direct interaction with dendritic cells. *J. Immunol.* 171:5140–5147.
17. Hermans, I.F., J.D. Silk, J. Yang, M.J. Palmowski, U. Gileadi, C. McCarthy, M. Salio, F. Ronchese, and V. Cerundolo. 2004. The VITAL assay: a versatile fluorometric technique for assessing CTL- and NKT-mediated cytotoxicity against multiple targets in vitro and in vivo. *J. Immunol. Methods.* 285:25–40.
18. Yu, K.O., J.S. Im, A. Molano, Y. Dutronc, P.A. Illarionov, C. Forestier, N. Fujiwara, I. Arias, S. Miyake, T. Yamamura, et al. 2005. Modulation of CD1d-restricted NKT cell responses by using *N*-acyl variants of α-galactosylceramides. *Proc. Natl. Acad. Sci. USA.* 102:3383–3388.
19. Wolf, P.R., and H.L. Ploegh. 1995. How MHC class II molecules acquire peptide cargo: biosynthesis and trafficking through the endocytic pathway. *Annu. Rev. Cell Dev. Biol.* 11:267–306.
20. Prigozy, T.I., O. Naidenko, P. Qasba, D. Elewaut, L. Brossay, A. Khurana, T. Natori, Y. Koezuka, A. Kulkarni, and M. Kronenberg. 2001. Glycolipid antigen processing for presentation by CD1d molecules. *Science.* 291:664–667.
21. Benlagha, K., T. Kyin, A. Beavis, L. Teyton, and A. Bendelac. 2002. A thymic precursor to the NK T cell lineage. *Science.* 296:553–555.
22. Pellicci, D.G., K.J. Hammond, A.P. Uldrich, A.G. Baxter, M.J. Smyth, and D.I. Godfrey. 2002. A natural killer T (NKT) cell developmental pathway involving a thymus-dependent NK1.1$^-$CD4$^+$ CD1d-dependent precursor stage. *J. Exp. Med.* 195:835–844.
23. Benlagha, K., D.G. Wei, J. Veiga, L. Teyton, and A. Bendelac. 2005. Characterization of the early stages of thymic NKT cell development. *J. Exp. Med.* 202:485–492.
24. Gapin, L., J.L. Matsuda, C.D. Surh, and M. Kronenberg. 2001. NKT cells derive from double-positive thymocytes that are positively selected by CD1d. *Nat. Immunol.* 2:971–978.
25. Matsuda, J.L., L. Gapin, S. Sidobre, W.C. Kieper, J.T. Tan, R. Ceredig, C.D. Surh, and M. Kronenberg. 2002. Homeostasis of Vα14i NKT cells. *Nat. Immunol.* 3:966–974.
26. Sagiv, Y., K. Hudspeth, J. Mattner, N. Schrantz, R.K. Stern, D. Zhou, P.B. Savage, L. Teyton, and A. Bendelac. 2006. Cutting edge: impaired glycosphingolipid trafficking and NKT cell development in mice lacking Niemann-Pick type C1 protein. *J. Immunol.* 177:26–30.
27. Zhou, D., C. Cantu III, Y. Sagiv, N. Schrantz, A.B. Kulkarni, X. Qi, D.J. Mahuran, C.R. Morales, G.A. Grabowski, K. Benlagha, et al. 2004. Editing of CD1d-bound lipid antigens by endosomal lipid transfer proteins. *Science.* 303:523–527.
28. Chen, C.S., M.C. Patterson, C.L. Wheatley, J.F. O'Brien, and R.E. Pagano. 1999. Broad screening test for sphingolipid-storage diseases. *Lancet.* 354:901–905.
29. Kolter, T., and K. Sandhoff. 2005. Principles of lysosomal membrane digestion: stimulation of sphingolipid degradation by sphingolipid activator proteins and anionic lysosomal lipids. *Annu. Rev. Cell Dev. Biol.* 21:81–103.
30. Balreira, A., L. Lacerda, C.S. Miranda, and F.A. Arosa. 2005. Evidence for a link between sphingolipid metabolism and expression of CD1d and MHC-class II: monocytes from Gaucher disease patients as a model. *Br. J. Haematol.* 129:667–676.
31. Yamanaka, S., M.D. Johnson, A. Grinberg, H. Westphal, J.N. Crawley, M. Taniike, K. Suzuki, and R.L. Proia. 1994. Targeted disruption of the Hexa gene results in mice with biochemical and pathologic features of Tay-Sachs disease. *Proc. Natl. Acad. Sci. USA.* 91:9975–9979.
32. Jeyakumar, M., D. Smith, E. Eliott-Smith, M. Cortina-Borja, G. Reinkensmeier, T.D. Butters, T. Lemm, K. Sandhoff, V.H. Perry, R.A. Dwek, and F.M. Platt. 2002. An inducible mouse model of late onset Tay-Sachs disease. *Neurobiol. Dis.* 10:201–210.
33. Sango, K., M.P. McDonald, J.N. Crawley, M.L. Mack, C.J. Tifft, E. Skop, C.M. Starr, A. Hoffmann, K. Sandhoff, K. Suzuki, and R.L. Proia. 1996. Mice lacking both subunits of lysosomal β-hexosaminidase display gangliosidosis and mucopolysaccharidosis. *Nat. Genet.* 14:348–352.
34. Ohshima, T., G.J. Murray, W.D. Swaim, G. Longenecker, J.M. Quirk, C.O. Cardarelli, Y. Sugimoto, I. Pastan, M.M. Gottesman, R.O. Brady, and A.B. Kulkarni. 1997. α-Galactosidase A deficient mice: a model of Fabry disease. *Proc. Natl. Acad. Sci. USA.* 94:2540–2544.
35. Hahn, C.N., M. del Pilar Martin, M. Schroder, M.T. Vanier, Y. Hara, K. Suzuki, and A. d'Azzo. 1997. Generalized CNS disease and massive GM1-ganglioside accumulation in mice defective in lysosomal acid β-galactosidase. *Hum. Mol. Genet.* 6:205–211.
36. Cui, J., T. Shin, T. Kawano, H. Sato, E. Kondo, I. Toura, Y. Kaneko, H. Koseki, M. Kanno, and M. Taniguchi. 1997. Requirement for Vα14 NKT cells in IL-12-mediated rejection of tumors. *Science.* 278:1623–1626.
37. Mendiratta, S.K., W.D. Martin, S. Hong, A. Boesteanu, S. Joyce, and L. Van Kaer. 1997. CD1d1 mutant mice are deficient in natural T cells that promptly produce IL-4. *Immunity.* 6:469–477.
38. Platt, F.M., G.B. Karlsson, and G.S. Jacob. 1992. Modulation of cell-surface transferrin receptor by the imino sugar *N*-butyldeoxynojirimycin. *Eur. J. Biochem.* 208:187–193.
39. Karadimitris, A., S. Gadola, M. Altamirano, D. Brown, A. Woolfson, P. Klenerman, J.L. Chen, Y. Koezuka, I.A. Roberts, D.A. Price, et al. 2001. Human CD1d-glycolipid tetramers generated by in vitro oxidative refolding chromatography. *Proc. Natl. Acad. Sci. USA.* 98:3294–3298.
40. Svennerholm, L., and P. Fredman. 1980. A procedure for the quantitative isolation of brain gangliosides. *Biochim. Biophys. Acta.* 617:97–109.
41. Neville, D.C., V. Coquard, D.A. Priestman, D.J. te Vruchte, D.J. Sillence, R.A. Dwek, F.M. Platt, and T.D. Butters. 2004. Analysis of fluorescently labeled glycosphingolipid-derived oligosaccharides following ceramide glycanase digestion and anthranilic acid labeling. *Anal. Biochem.*331:275–282.